

Search for New Particles Decaying to Dijets at CDF

F. Abe,¹⁶ H. Akimoto,³⁵ A. Akopian,³⁰ M. G. Albrow,⁷ S. R. Amendolia,²⁶ D. Amidei,¹⁹ J. Antos,³² S. Aota,³⁵ G. Apollinari,³⁰ T. Asakawa,³⁵ W. Ashmanskas,¹⁷ M. Atac,⁷ F. Azfar,²⁵ P. Azzi-Bacchetta,²⁴ N. Bacchetta,²⁴ W. Badgett,¹⁹ S. Bagdasarov,³⁰ M. W. Bailey,²¹ J. Bao,³⁸ P. de Barbaro,²⁹ A. Barbaro-Galtieri,¹⁷ V. E. Barnes,²⁸ B. A. Barnett,¹⁵ M. Barone,⁹ E. Barzi,⁹ G. Bauer,¹⁸ T. Baumann,¹¹ F. Bedeschi,²⁶ S. Behrends,³ S. Belforte,²⁶ G. Bellettini,²⁶ J. Bellinger,³⁷ D. Benjamin,³⁴ J. Benlloch,¹⁸ J. Bensinger,³ D. Benton,²⁵ A. Beretvas,⁷ J. P. Berge,⁷ J. Berryhill,⁵ S. Bertolucci,⁹ B. Bevensee,²⁵ A. Bhatti,³⁰ K. Biery,⁷ M. Binkley,⁷ D. Bisello,²⁴ R. E. Blair,¹ C. Blocker,³ A. Bodek,²⁹ W. Bokhari,¹⁸ V. Bolognesi,² G. Bolla,²⁸ D. Bortoletto,²⁸ J. Boudreau,²⁷ L. Breccia,² C. Bromberg,²⁰ N. Bruner,²¹ E. Buckley-Geer,⁷ H. S. Budd,²⁹ K. Burkett,¹⁹ G. Busetto,²⁴ A. Byon-Wagner,⁷ K. L. Byrum,¹ J. Cammerata,¹⁵ C. Campagnari,⁷ M. Campbell,¹⁹ A. Caner,²⁶ W. Carithers,¹⁷ D. Carlsmith,³⁷ A. Castro,²⁴ D. Cauz,²⁶ Y. Cen,²⁹ F. Cervelli,²⁶ P. S. Chang,³² P. T. Chang,³² H. Y. Chao,³² J. Chapman,¹⁹ M. - T. Cheng,³² G. Chiarelli,²⁶ T. Chikamatsu,³⁵ C. N. Chiou,³² L. Christofek,¹³ S. Cihangir,⁷ A. G. Clark,¹⁰ M. Cobal,²⁶ E. Cocca,²⁶ M. Contreras,⁵ J. Conway,³¹ J. Cooper,⁷ M. Cordelli,⁹ C. Couyoumtzelis,¹⁰ D. Crane,¹ D. Cronin-Hennessy,⁶ R. Culbertson,⁵ T. Daniels,¹⁸ F. DeJongh,⁷ S. Delchamps,⁷ S. Dell'Agnello,²⁶ M. Dell'Orso,²⁶ R. Demina,⁷ L. Demortier,³⁰ M. Deninno,² P. F. Derwent,⁷ T. Devlin,³¹ J. R. Dittmann,⁶ S. Donati,²⁶ J. Done,³³ T. Dorigo,²⁴ A. Dunn,¹⁹ N. Eddy,¹⁹ K. Einsweiler,¹⁷ J. E. Elias,⁷ R. Ely,¹⁷ E. Engels, Jr.,²⁷ D. Errede,¹³ S. Errede,¹³ Q. Fan,²⁹ G. Feild,³⁸ C. Ferretti,²⁶ I. Fiori,² B. Flaughier,⁷ L. Fortney,⁶ G. W. Foster,⁷ M. Franklin,¹¹ M. Frautschi,³⁴ J. Freeman,⁷ J. Friedman,¹⁸ H. Frisch,⁵ Y. Fukui,¹⁶ S. Funaki,³⁵ S. Galeotti,²⁶ M. Gallinaro,²⁵ O. Ganel,³⁴ M. Garcia-Sciveres,¹⁷ A. F. Garfinkel,²⁸ C. Gay,¹¹ S. Geer,⁷ D. W. Gerdes,¹⁵ P. Giannetti,²⁶ N. Giokaris,³⁰ P. Giromini,⁹ G. Giusti,²⁶ L. Gladney,²⁵ D. Glenzinski,¹⁵ M. Gold,²¹ J. Gonzalez,²⁵ A. Gordon,¹¹ A. T. Goshaw,⁶ Y. Gotra,²⁴ K. Goulianios,³⁰ H. Grassmann,²⁶ L. Groer,³¹ C. Grossi-Pilcher,⁵ G. Guillian,¹⁹ R. S. Guo,³² C. Haber,¹⁷ E. Hafen,¹⁸ S. R. Hahn,⁷ R. Hamilton,¹¹ R. Handler,³⁷ R. M. Hans,³⁸ F. Happacher,⁹ K. Hara,³⁵ A. D. Hardman,²⁸ B. Harral,²⁵ R. M. Harris,⁷ S. A. Hauger,⁶ J. Hauser,⁴ C. Hawk,³¹ E. Hayashi,³⁵ J. Heinrich,²⁵ K. D. Hoffman,²⁸ M. Hohlmann,⁵ C. Holdk,²⁵ R. Hollebeek,²⁵ L. Holloway,¹³ A. Hölscher,¹⁴ S. Hong,¹⁹ G. Houk,²⁵ P. Hu,²⁷ B. T. Huffman,²⁷ R. Hughes,²² J. Huston,²⁰ J. Huth,¹¹ J. Hylen,⁷ H. Ikeda,³⁵ M. Incagli,²⁶ J. Incandela,⁷ G. Introzzi,²⁶ J. Iwai,³⁵ Y. Iwata,¹² H. Jensen,⁷ U. Joshi,⁷ R. W. Kadel,¹⁷ E. Kajfasz,²⁴ H. Kambara,¹⁰ T. Kamon,³³ T. Kaneko,³⁵ K. Karr,³⁶ H. Kasha,³⁸ Y. Kato,²³ T. A. Keaffaber,²⁸ L. Keeble,⁹ K. Kelley,¹⁸ R. D. Kennedy,⁷ R. Kephart,⁷ P. Kesten,¹⁷ D. Kestenbaum,¹¹ R. M. Keup,¹³ H. Keutelian,⁷ F. Keyvan,⁴ B. Kharadria,¹³ B. J. Kim,²⁹ D. H. Kim,^{7a}

H. S. Kim,¹⁴ S. B. Kim,¹⁹ S. H. Kim,³⁵ Y. K. Kim,¹⁷ L. Kirsch,³ P. Koehn,²⁹ K. Kondo,³⁵ J. Konigsberg,⁸ S. Kopp,⁵ K. Kordas,¹⁴ A. Korytov,⁸ W. Koska,⁷ E. Kovacs,^{7a} W. Kowald,⁶ M. Krasberg,¹⁹ J. Kroll,⁷ M. Kruse,²⁹ T. Kuwabara,³⁵ S. E. Kuhlmann,¹ E. Kuns,³¹ A. T. Laasanen,²⁸ S. Lami,²⁶ S. Lammel,⁷ J. I. Lamoureux,³ T. LeCompte,¹ S. Leone,²⁶ J. D. Lewis,⁷ P. Limon,⁷ M. Lindgren,⁴ T. M. Liss,¹³ N. Lockyer,²⁵ O. Long,²⁵ C. Loomis,³¹ M. Loretta,²⁴ J. Lu,³³ D. Lucchesi,²⁶ P. Lukens,⁷ S. Lusin,³⁷ J. Lys,¹⁷ K. Maeshima,⁷ A. Maghakian,³⁰ P. Maksimovic,¹⁸ M. Mangano,²⁶ J. Mansour,²⁰ M. Mariotti,²⁴ J. P. Marriner,⁷ A. Martin,³⁸ J. A. J. Matthews,²¹ R. Mattingly,¹⁸ P. McIntyre,³³ P. Melese,³⁰ A. Menzione,²⁶ E. Meschi,²⁶ S. Metzler,²⁵ C. Miao,¹⁹ T. Miao,⁷ G. Michail,¹¹ R. Miller,²⁰ H. Minato,³⁵ S. Miscetti,⁹ M. Mishina,¹⁶ H. Mitsushio,³⁵ T. Miyamoto,³⁵ S. Miyashita,³⁵ N. Moggi,²⁶ Y. Morita,¹⁶ J. Mueller,²⁷ A. Mukherjee,⁷ T. Muller,⁴ P. Murat,²⁶ H. Nakada,³⁵ I. Nakano,³⁵ C. Nelson,⁷ D. Neuberger,⁴ C. Newman-Holmes,⁷ C.-Y. Ngan,¹⁸ M. Ninomiya,³⁵ L. Nodulman,¹ S. H. Oh,⁶ K. E. Ohl,³⁸ T. Ohmoto,¹² T. Ohsugi,¹² R. Oishi,³⁵ M. Okabe,³⁵ T. Okusawa,²³ R. Oliveira,²⁵ J. Olsen,³⁷ C. Pagliarone,²⁶ R. Paoletti,²⁶ V. Papadimitriou,³⁴ S. P. Pappas,³⁸ N. Parashar,²⁶ S. Park,⁷ A. Parri,⁹ J. Patrick,⁷ G. Paulette,²⁶ M. Paulini,¹⁷ A. Perazzo,²⁶ L. Pescara,²⁴ M. D. Peters,¹⁷ T. J. Phillips,⁶ G. Piacentino,²⁶ M. Pillai,²⁹ K. T. Pitts,⁷ R. Plunkett,⁷ L. Pondrom,³⁷ J. Proudfoot,¹ F. Ptohos,¹¹ G. Punzi,²⁶ K. Ragan,¹⁴ D. Reher,¹⁷ A. Ribon,²⁴ F. Rimondi,² L. Ristori,²⁶ W. J. Robertson,⁶ T. Rodrigo,²⁶ S. Rolli,³⁶ J. Romano,⁵ L. Rosenson,¹⁸ R. Roser,¹³ W. K. Sakumoto,²⁹ D. Saltzberg,⁵ A. Sansoni,⁹ L. Santi,²⁶ H. Sato,³⁵ P. Schlabach,⁷ E. E. Schmidt,⁷ M. P. Schmidt,³⁸ A. Scribano,²⁶ S. Segler,⁷ S. Seidel,²¹ Y. Seiya,³⁵ G. Sganos,¹⁴ M. D. Shapiro,¹⁷ N. M. Shaw,²⁸ Q. Shen,²⁸ P. F. Shepard,²⁷ M. Shimojima,³⁵ M. Shochet,⁵ J. Siegrist,¹⁷ A. Sill,³⁴ P. Sinervo,¹⁴ P. Singh,²⁷ J. Skarha,¹⁵ K. Sliwa,³⁶ F. D. Snider,¹⁵ T. Song,¹⁹ J. Spalding,⁷ T. Speer,¹⁰ P. Sphicas,¹⁸ F. Spinella,²⁶ M. Spiropulu,¹¹ L. Spiegel,⁷ L. Stanco,²⁴ J. Steele,³⁷ A. Stefanini,²⁶ K. Strahl,¹⁴ J. Strait,⁷ R. Ströhmer,^{7a} D. Stuart,⁷ G. Sullivan,⁵ A. Soumarokov,³² K. Sumorok,¹⁸ J. Suzuki,³⁵ T. Takada,³⁵ T. Takahashi,²³ T. Takano,³⁵ K. Takikawa,³⁵ N. Tamura,¹² B. Tannenbaum,²¹ F. Tartarelli,²⁶ W. Taylor,¹⁴ P. K. Teng,³² Y. Teramoto,²³ S. Tether,¹⁸ D. Theriot,⁷ T. L. Thomas,²¹ R. Thun,¹⁹ M. Timko,³⁶ P. Tipton,²⁹ A. Titov,³⁰ S. Tkaczyk,⁷ D. Toback,⁵ K. Tollefson,²⁹ A. Tollestrup,⁷ H. Toyoda,²³ W. Trischuk,¹⁴ J. F. de Troconiz,¹¹ S. Truitt,¹⁹ J. Tseng,¹⁸ N. Turini,²⁶ T. Uchida,³⁵ N. Uemura,³⁵ F. Ukegawa,²⁵ G. Unal,²⁵ J. Valls,^{7a} S. C. van den Brink,²⁷ S. Vejcik, III,¹⁹ G. Velev,²⁶ R. Vidal,⁷ R. Vilar,^{7a} M. Vondracek,¹³ D. Vucinic,¹⁸ R. G. Wagner,¹ R. L. Wagner,⁷ J. Wahl,⁵ N. B. Wallace,²⁶ A. M. Walsh,³¹ C. Wang,⁶ C. H. Wang,³² J. Wang,⁵ M. J. Wang,³² Q. F. Wang,³⁰ A. Warburton,¹⁴ T. Watts,³¹ R. Webb,³³ C. Wei,⁶ C. Wendt,³⁷ H. Wenzel,¹⁷ W. C. Wester, III,⁷ A. B. Wicklund,¹ E. Wicklund,⁷ R. Wilkinson,²⁵ H. H. Williams,²⁵ P. Wilson,⁵ B. L. Winer,²² D. Winn,¹⁹ D. Wolinski,¹⁹ J. Wolinski,²⁰ S. Worm,²¹ X. Wu,¹⁰ J. Wyss,²⁴ A. Yagil,⁷ W. Yao,¹⁷ K. Yasuoka,³⁵ Y. Ye,¹⁴ G. P. Yeh,⁷ P. Yeh,³² M. Yin,⁶ J. Yoh,⁷ C. Yosef,²⁰ T. Yoshida,²³ D. Yovanovitch,⁷ I. Yu,⁷ L. Yu,²¹ J. C. Yun,⁷ A. Zanetti,²⁶ F. Zetti,²⁶ L. Zhang,³⁷ W. Zhang,²⁵ and S. Zucchelli²

(CDF Collaboration)

- ¹ Argonne National Laboratory, Argonne, Illinois 60439
² Istituto Nazionale di Fisica Nucleare, University of Bologna, I-40127 Bologna, Italy
³ Brandeis University, Waltham, Massachusetts 02264
⁴ University of California at Los Angeles, Los Angeles, California 90024
⁵ University of Chicago, Chicago, Illinois 60638
⁶ Duke University, Durham, North Carolina 28708
⁷ Fermi National Accelerator Laboratory, Batavia, Illinois 60510
⁸ University of Florida, Gainesville, FL 33611
⁹ Laboratori Nazionali di Frascati, Istituto Nazionale di Fisica Nucleare, I-00044 Frascati, Italy
¹⁰ University of Geneva, CH-1211 Geneva 4, Switzerland
¹¹ Harvard University, Cambridge, Massachusetts 02138
¹² Hiroshima University, Higashi-Hiroshima 724, Japan
¹³ University of Illinois, Urbana, Illinois 61801
¹⁴ Institute of Particle Physics, McGill University, Montreal H3A 2T8, and University of Toronto, Toronto M5S 1A7, Canada
¹⁵ The Johns Hopkins University, Baltimore, Maryland 21218
¹⁶ National Laboratory for High Energy Physics (KEK), Tsukuba, Ibaraki 315, Japan
¹⁷ Ernest Orlando Lawrence Berkeley National Laboratory, Berkeley, California 94720
¹⁸ Massachusetts Institute of Technology, Cambridge, Massachusetts 02139
¹⁹ University of Michigan, Ann Arbor, Michigan 48109
²⁰ Michigan State University, East Lansing, Michigan 48824
²¹ University of New Mexico, Albuquerque, New Mexico 87132
²² The Ohio State University, Columbus, OH 43320
²³ Osaka City University, Osaka 588, Japan
²⁴ Universita di Padova, Istituto Nazionale di Fisica Nucleare, Sezione di Padova, I-36132 Padova, Italy
²⁵ University of Pennsylvania, Philadelphia, Pennsylvania 19104
²⁶ Istituto Nazionale di Fisica Nucleare, University and Scuola Normale Superiore of Pisa, I-56100 Pisa, Italy
²⁷ University of Pittsburgh, Pittsburgh, Pennsylvania 15270
²⁸ Purdue University, West Lafayette, Indiana 47907
²⁹ University of Rochester, Rochester, New York 14628
³⁰ Rockefeller University, New York, New York 10021
³¹ Rutgers University, Piscataway, New Jersey 08854
³² Academia Sinica, Taipei, Taiwan 11530, Republic of China
³³ Texas A&M University, College Station, Texas 77843
³⁴ Texas Tech University, Lubbock, Texas 79409
³⁵ University of Tsukuba, Tsukuba, Ibaraki 315, Japan
³⁶ Tufts University, Medford, Massachusetts 02155
³⁷ University of Wisconsin, Madison, Wisconsin 53806
³⁸ Yale University, New Haven, Connecticut 06511

Abstract

We have used 106 pb^{-1} of data collected with the Collider Detector at Fermilab to search for new particles decaying to dijets. We exclude at the 95% confidence level models containing the following new particles: axigluons and flavor universal colorons with mass between 200 and $980 \text{ GeV}/c^2$, excited quarks with mass between 80 and $570 \text{ GeV}/c^2$ and between 580 and $760 \text{ GeV}/c^2$, color octet technirhos with mass between 260 and $480 \text{ GeV}/c^2$, W' bosons with mass between 300 and $420 \text{ GeV}/c^2$, and E_6 diquarks with mass between 290 and $420 \text{ GeV}/c^2$.

PACS numbers: 13.85.Rm, 12.38.Qk, 14.70.Pw, 14.80.-j

In this paper we extend a previous search [1] for narrow resonances in the dijet mass spectrum in $p\bar{p}$ collisions at a center-of-mass energy $\sqrt{s} = 1.8 \text{ TeV}$. The previous search used 19 pb^{-1} of data collected in 1992-93 from run 1A of the Tevatron. This search uses 106 pb^{-1} of data collected in 1992-95 from both run 1A and run 1B, and significantly extends our sensitivity to new particles.

As before, we perform both a general search for narrow resonances and a specific search for axigluons [2], excited quarks [3], color octet technirhos [4], W' , Z' [5], and E_6 diquarks [6]. In addition, the flavor universal coloron [7], a hypothesized massive gluon which couples equally to all quarks, is considered together with axigluons. The cross section for the coloron is always greater than or equal to that of the axigluon,

so our axigluon limits will apply to the coloron as well. In models of supersymmetry in which the gluino is lighter than $5 \text{ GeV}/c^2$, there can be dijet resonances resulting from squark decay [8, 9]. We do not consider this model, since data from both our previous search and from a preliminary version of the present search has already been used to exclude a range of squark masses in the light gluino scenario [8, 9].

A detailed description of the Collider Detector at Fermilab (CDF) can be found elsewhere [10]. We use a coordinate system with the z axis along the proton beam, transverse coordinate perpendicular to the beam, azimuthal angle ϕ , polar angle θ , and pseudorapidity $\eta = -\ln \tan(\theta/2)$. Jets are reconstructed as localized energy depositions in the CDF calorimeters that are arranged in a projective tower geometry. The jet energy E is defined as the scalar sum of the calorimeter tower energies inside a cone of radius $R = \sqrt{(\Delta\eta)^2 + (\Delta\phi)^2} = 0.7$, centered on the jet direction. The jet momentum \vec{P} is the corresponding vector sum: $\vec{P} = \sum E_i \hat{u}_i$ with \hat{u}_i being the unit vector pointing from the interaction point to the energy deposition E_i inside the same cone. E and \vec{P} are corrected for calorimeter non-linearities, energy lost in uninstrumented regions of the detector and outside the clustering cone, and energy gained from the underlying event and multiple $p\bar{p}$ interactions. The jet energy corrections increase the jet energies on average by roughly 24% (19%) for 50 GeV (500 GeV) jets. Full details of jet reconstruction and jet energy corrections at CDF can be found elsewhere [11].

We define the dijet system as the two jets with the highest transverse momentum in an event (leading jets) and define the dijet mass $m = \sqrt{(E_1 + E_2)^2 - (\vec{P}_1 + \vec{P}_2)^2}$.

The dijet mass resolution is approximately 10% for dijet mass above 150 GeV/c².

Our data sample was obtained using four triggers that required at least one jet with uncorrected cluster transverse energies of 20, 50, 70 and 100 GeV, respectively. After jet energy corrections these trigger samples were used to measure the dijet mass spectrum above 180, 241, 292 and 388 GeV/c², respectively. At these mass thresholds the trigger efficiencies were greater than 95%. The four data samples corresponded to integrated luminosities of 0.126, 2.84, 14.1 and 106 pb⁻¹ after prescaling. Offline we required that both jets have pseudorapidity $|\eta| < 2$ and a scattering angle in the dijet center-of-mass frame $|\cos \theta^*| = |\tanh[(\eta_1 - \eta_2)/2]| < 2/3$. The $\cos \theta^*$ requirement provides uniform acceptance as a function of mass and reduces the QCD background which peaks at $|\cos \theta^*| = 1$. To utilize the projective nature of the calorimeter towers, the z position of the event vertex was required to be within 60 cm of the center of the detector; this cut removed 7% of the events. Backgrounds from cosmic-rays, beam halo, and detector noise were removed with the cuts reported previously [1], and residual backgrounds were removed by requiring that the total observed energy be less than 2 TeV.

In Fig. 1 we present the inclusive dijet mass distribution for $p\bar{p} \rightarrow 2 \text{ jets} + X$, where X can be anything including additional jets. The dijet mass distribution has been corrected for trigger and z vertex inefficiencies. We plot the differential cross section versus the mean dijet mass in bins of width approximately equal to the dijet mass resolution (RMS~10%). The data are compared to a QCD prediction from the PYTHIA Monte Carlo [12] and a simulation of the CDF detector. The cross

section predicted by the QCD simulation, using CTEQ2L parton distributions [13] and a renormalization scale $\mu = P_T$, is normalized to the data in the first 6 bins ($180 < m < 321 \text{ GeV}/c^2$) by dividing the simulation by a factor of 0.66. In Fig. 1 the horizontal lines on the data points indicate the bin width, the same width in data and simulation. The points are plotted at the mean mass, calculated independently for data and simulation.

We note that the data is above the QCD simulation at high mass. In a previous paper [14], we reported a similar effect in the fully corrected inclusive jet transverse energy distribution compared to an $O(\alpha_s^3)$ parton level QCD calculation. Unlike the inclusive jet analysis, here we do not deconvolute the mass distribution for the effects of detector resolution, and instead compare the data directly to QCD plus a CDF detector simulation. In our previous dijet mass search the excess was not as noticeable because we normalized the simulation to the data on average, while here we normalize to the low mass end as described above. In another paper [15] we have studied the dijet angular distributions and find them to be in good agreement with QCD in all regions, including at high mass. The source of the high dijet mass and high jet transverse energy excess is not yet fully understood. Candidate explanations within the Standard Model include a larger than expected gluon distribution of the proton [16] or large QCD corrections from resummation [17]. As in our previous search [1], we do not use QCD calculations to determine the background to new particles, but merely use the data itself to fit for the background.

To search for resonances we fit the data with the parameterization $d\sigma/dm =$

$A(1 - m/\sqrt{s} + Cm^2/s)^N/m^P$ with parameters A, C, N and P. In the run 1A search [1] the term Cm^2/s was not used because fewer parameters were needed to fit the lower statistics sample. With the higher statistics in this sample the extra term Cm^2/s was needed to obtain an acceptable fit. This parameterization gives an adequate description of both the observed distribution ($\chi^2/DF = 1.49$) and the QCD prediction ($\chi^2/DF = 0.85$). Figure 1 shows the background fit on a logarithmic scale, and Fig. 2 shows the fractional difference between the data and background fit on a linear scale.

Figures 1 and 2 also show the predicted line shape for excited quarks (q^*) using the PYTHIA Monte Carlo [12] and a CDF detector simulation. If excited quarks were produced in $p\bar{p}$ collisions, their production and decay to dijets would proceed via the process $qg \rightarrow q^* \rightarrow qg$. The mass resolution is dominated by a Gaussian distribution (RMS $\sim 10\%$) from jet energy resolution and a long tail towards low mass from QCD radiation. Since the natural width of a q^* is significantly smaller than the measured width, the q^* mass resonance curves in Figs. 1 and 2 were used to model the shape of all narrow resonances decaying to dijets.

There is no statistically significant evidence for a dijet mass resonance, which should appear in at least two neighboring bins above the background fit. We note that in the region of $550 \text{ GeV}/c^2$ there is a single bin which is 2.6 standard deviations above the fit; however, this region is not well fit by a new resonance because the number of events in neighboring bins is too low. When we fit the data to both a $550 \text{ GeV}/c^2$ resonance and a smooth background we find that the upward fluctuation in the data is significantly narrower than expected for a resonance.

Systematic uncertainties on the cross section for observing a new particle in the CDF detector are shown in Fig. 2. Each systematic uncertainty on the fitted signal cross section was determined by varying the source of uncertainty by $\pm 1\sigma$ and refitting. In decreasing order of importance the sources of uncertainty are the 5% jet energy scale uncertainty, low mass data, the background parameterization, QCD radiation's effect on the mass resonance line shape, trigger efficiency, jet energy resolution, relative jet energy corrections between different parts of the CDF calorimeter, energy scale of run 1A with respect to run 1B, luminosity and efficiency. For example, at 600 GeV/c^2 reducing the jet energy by 5% centers the resonance on an upward fluctuation, and increases the fitted signal by 225%. The low mass data uncertainty, listed above, is because the background fit gets significantly worse when data between 150 and 180 GeV/c^2 are included. The larger number of interactions per crossing in run 1B increases the uncertainty on the lower mass data, so we start the mass distribution at 180 GeV/c^2 . However, since this mass range was included in run 1A, the effect of adding the low mass data is included as a systematic for run 1A plus run 1B.

The total systematic uncertainty was found by adding the individual sources in quadrature. In this analysis the relative systematic error is larger than it was in the previous analysis: the total run 1A and 1B systematics range from 40% to 300% of the cross section while the run 1A systematics ranged from 30% to 120%. This is not because the absolute systematics have significantly increased, but instead because the size of the signal we are statistically sensitive to has decreased by over a factor of two, so now the systematics have a larger relative effect. This is particularly true at

masses near upward fluctuations in the data.

In the absence of conclusive evidence for new physics we proceed to set upper limits on the cross section for new particles. For each value of new particle mass in 50 GeV/c^2 steps from 200 to 1150 GeV/c^2 , we perform a binned maximum likelihood fit of the data to the background parameterization and the mass resonance shape. We convolute each of the 20 likelihood distributions with the corresponding total Gaussian systematic uncertainty, and find the 95% confidence level (CL) upper limit presented in Table I.

In Fig. 3 we plot our measured upper limit on the cross section times branching ratio for a new particle decaying to dijets as a function of new particle mass in 50 GeV/c^2 steps. The points are connected by a smooth curve, which is an estimate of the upper limit in between the measured points. The limit is compared to lowest order theoretical predictions for the cross section times branching ratio for new particles decaying to dijets [1]. New particle decay angular distributions are included in the calculations, and we required $|\eta| < 2$ and $|\cos\theta^*| < 2/3$ for all predictions. For axigluons (or flavor universal colorons) we exclude the mass range $200 < M_A < 980 \text{ GeV}/c^2$, extending the previous CDF exclusions of $120 < M_A < 870 \text{ GeV}/c^2$ [1]. For excited quarks we exclude the mass ranges $200 < M^* < 520$ and $580 < M^* < 760 \text{ GeV}/c^2$, significantly extending the previous CDF exclusion of $80 < M^* < 570 \text{ GeV}/c^2$ [1, 18]. The D0 collaboration has performed a preliminary search for excited quarks and exclude the mass range $200 < M^* < 720 \text{ GeV}/c^2$ [19]. These exclusions are for Standard Model couplings ($f = f' = f_s = 1$). For smaller couplings, the new

excluded region in the coupling [3] vs. mass plane is shown in Fig. 4 compared to previous excluded regions. For color octet technirhos (ρ_T) we exclude the mass range $260 < M_{\rho_T} < 470 \text{ GeV}/c^2$, extending to lower mass the previous CDF exclusion of $320 < M_{\rho_T} < 480 \text{ GeV}/c^2$ [1]. For the first time we exclude the hadronic decays of the new gauge boson W' in the mass range $300 < M_{W'} < 420 \text{ GeV}/c^2$. Also for the first time we exclude E_6 diquarks in the mass range $290 < M_{E_6} < 420 \text{ GeV}/c^2$. The cross section for hadronic decays of Z' is too small to exclude.

In conclusion, the measured dijet mass spectrum does not contain evidence for a mass peak from a new particle resonance. We have presented model independent limits on the cross section for a narrow resonance, and set specific mass limits on axigluons, flavor universal colorons, excited quarks, color octet technirhos, new charged gauge bosons, and E_6 diquarks.

We thank the Fermilab staff and the technical staffs of the participating institutions for their vital contributions. This work was supported by the U.S. Department of Energy and National Science Foundation; the Italian Istituto Nazionale di Fisica Nucleare; the Ministry of Education, Science and Culture of Japan; the Natural Sciences and Engineering Research Council of Canada; the National Science Council of the Republic of China; and the A. P. Sloan Foundation.

References

- [1] F. Abe *et al.*, Phys. Rev. Lett. **74**, 3538 (1995).

- [2] P. Frampton and S. Glashow, Phys. Lett. **B190**, 157 (1987); J. Bagger, C. Schmidt and S. King, Phys. Rev. **D37**, 1188 (1988).
- [3] U. Baur, I. Hinchliffe and D. Zeppenfeld, Int. J. Mod. Phys **A2**, 1285 (1987); U. Baur, M. Spira and P. Zerwas, Phys. Rev. **D42**, 815 (1990).
- [4] K. Lane and M. Ramana, Phys. Rev. **D44**, 2678 (1991); E. Eichten and K. Lane, Phys. Lett. **B327**, 129 (1994).
- [5] F. Abe *et al.*, Phys. Rev. Lett. **74**, 2900 (1995) and Phys. Rev. **D51**, R949 (1995), and references therein.
- [6] J. Hewett and T. Rizzo, Phys. Rep. **183**, 193 (1989) and references therein.
- [7] R. S. Chivukula, A. G. Cohen, and E. Simmons, Phys. Lett. **B380**, 92 (1996); E. Simmons, Phys. Rev. **D55**, 1678 (1997).
- [8] I. Terekhov and L. Clavelli, Phys. Lett. **B385**, 139 (1996).
- [9] J. Hewett, T. Rizzo and M. Doncheski, SLAC-PUB-7372 (1996).
- [10] F. Abe *et al.*, Nucl. Instrum. and Methods **A271**, 387 (1988).
- [11] F. Abe *et al.*, Phys. Rev. **D45**, 1448 (1992).
- [12] PYTHIA V5.6 by T. Sjostrand, CERN-TH-7112/93, Feb 1994.
- [13] J. Botts *et al.*, Phys. Lett. **B304**, 159 (1993).
- [14] F. Abe *et al.*, Phys. Rev. Lett. **77**, 438 (1996).

- [15] F. Abe *et al.*, Phys. Rev. Lett. **77**, 5336 (1996).
- [16] H. L. Lai *et al.*, MSUHEP-60426, hep-ph/9606399 submitted to Phys. Rev. D.
- [17] S. Catani *et al.*, Nucl. Phys. **B478**, 273 (1996).
- [18] F. Abe *et al.*, Phys. Rev. Lett. **72**, 3004 (1994).
- [19] I. Bertram for the D0 Collaboration, Fermilab-Conf-96/389-E (1996).
- [20] D. Decamp *et al.*, Phys. Rep. **216**, 253 (1992); J. Alitti *et al.*, Nucl. Phys. **B400**, 3 (1993).

Mass (GeV/c ²)	95% CL $\sigma \cdot B$ (pb)	Mass (GeV/c ²)	95% CL $\sigma \cdot B$ (pb)
200	1.3×10^4	700	1.3×10^0
250	7.6×10^2	750	8.6×10^{-1}
300	7.7×10^1	800	8.4×10^{-1}
350	3.8×10^1	850	9.3×10^{-1}
400	1.6×10^1	900	9.5×10^{-1}
450	1.5×10^1	950	7.4×10^{-1}
500	3.1×10^1	1000	5.6×10^{-1}
550	2.1×10^1	1050	4.1×10^{-1}
600	8.3×10^0	1100	3.1×10^{-1}
650	2.9×10^0	1150	1.2×10^{-1}

Table I: As a function of new particle mass we list our 95% CL upper limit on cross section times branching ratio for narrow resonances decaying to dijets. The limit applies to the kinematic range where both jets have pseudorapidity $|\eta| < 2.0$ and where the dijet system satisfies $|\cos \theta^*| < 2/3$.

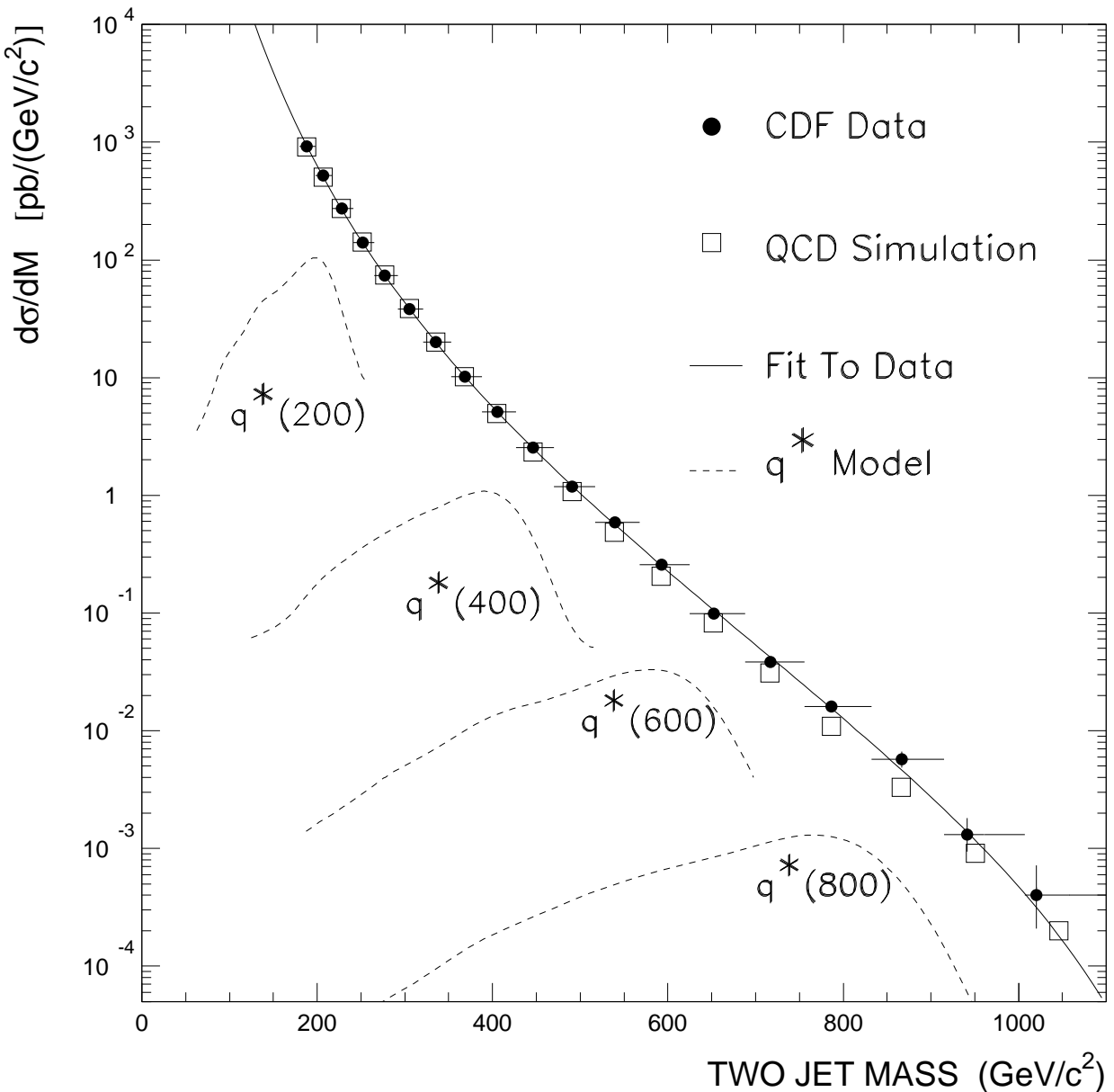


Figure 1: The dijet mass distribution (circles) compared to a QCD simulation (boxes) and fit to a smooth parameterization (solid curve). Also shown are simulations of excited quark signals in the CDF detector (dashed curves). In the data and simulations we require that both jets have pseudorapidity $|\eta| < 2.0$ and that the dijet system satisfies $|\cos \theta^*| < 2/3$.

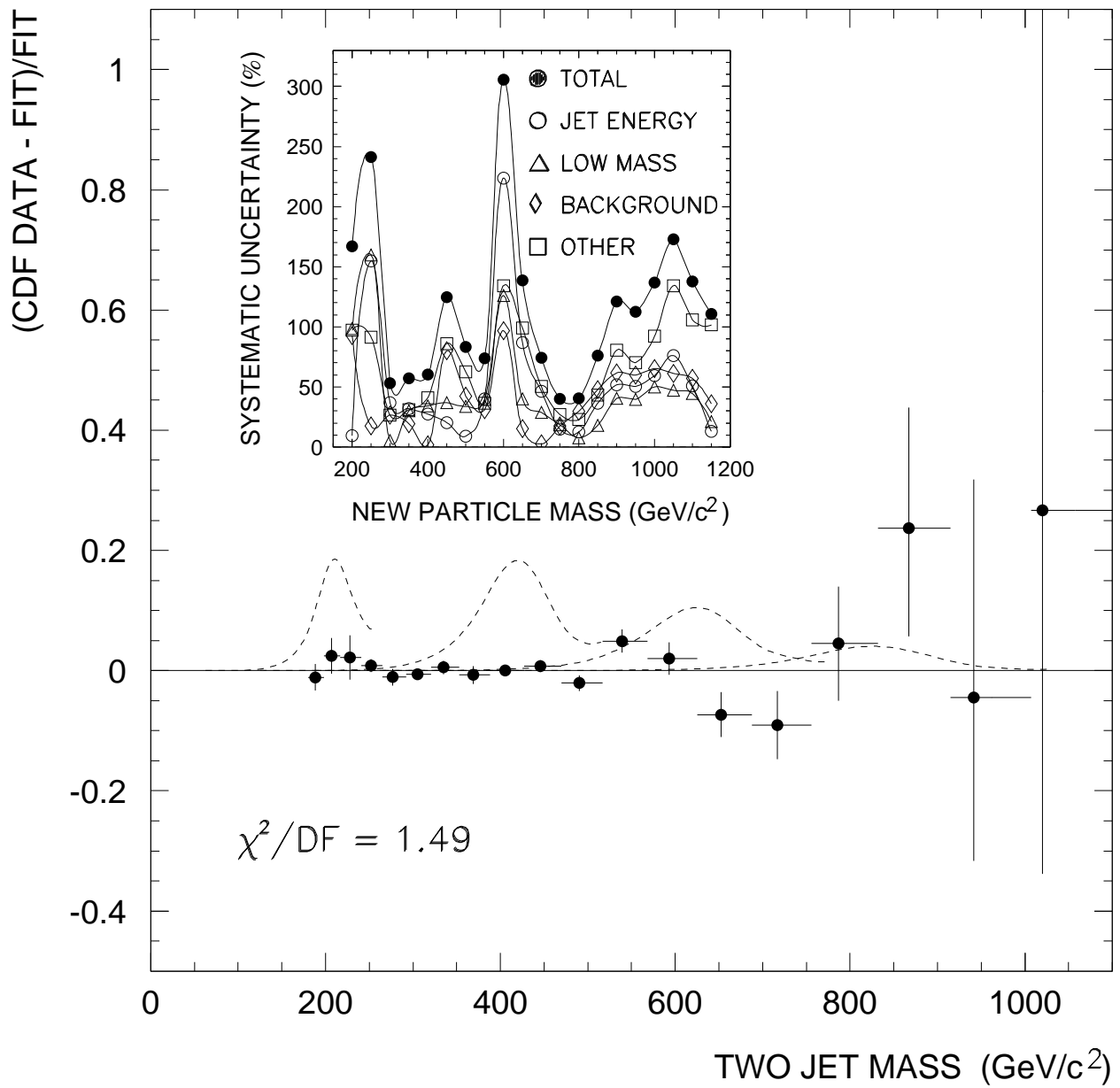


Figure 2: The fractional difference between the dijet mass distribution (points) and a smooth background fit (solid line) is compared to simulations of excited quark signals in the CDF detector (dashed curves). The inset shows the systematic uncertainty for a new particle signal (see text).

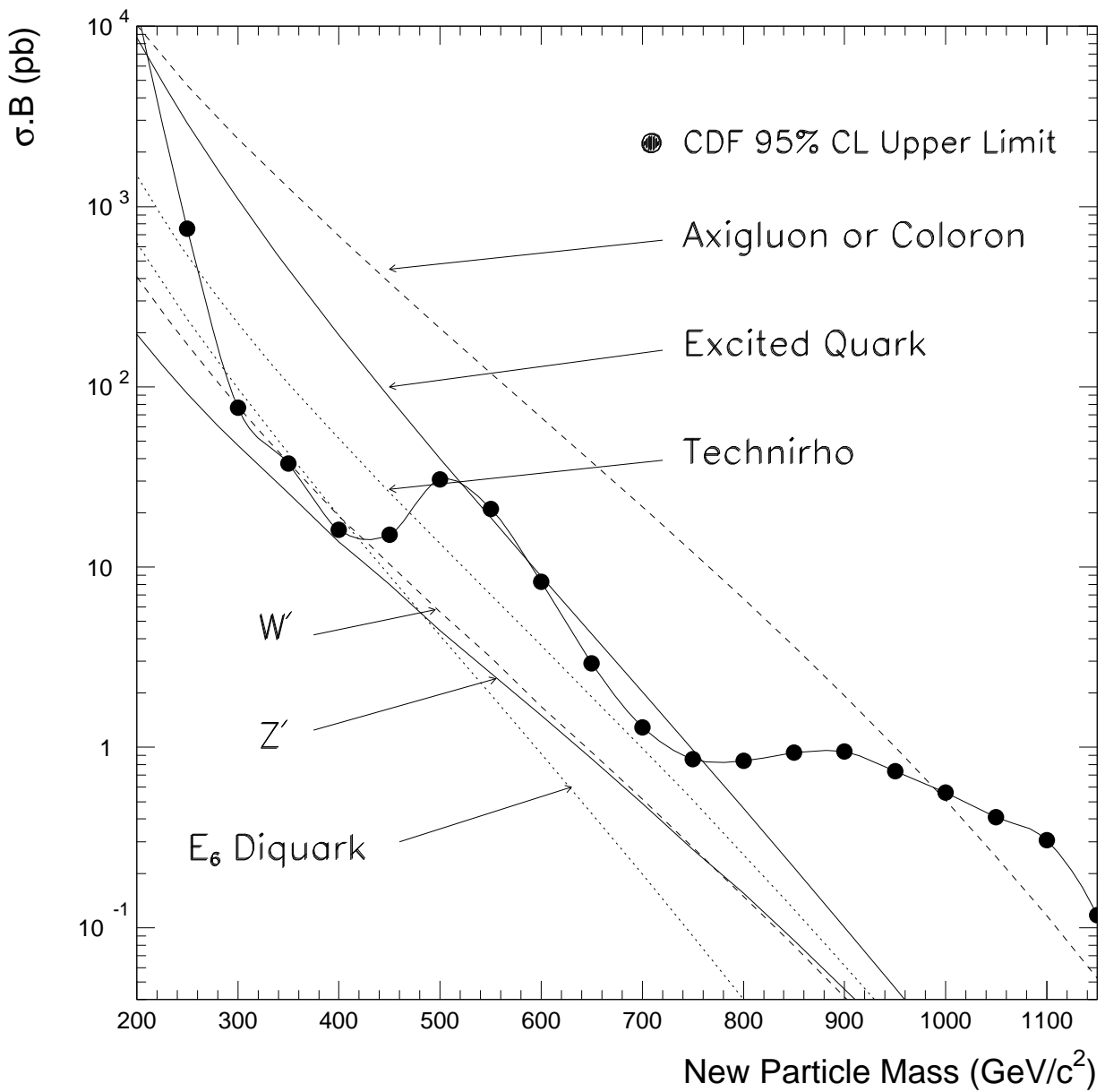


Figure 3: The upper limit on the cross section times branching ratio for new particles decaying to dijets (points) is compared to theoretical predictions for axigluons [2], flavor universal colorons [7], excited quarks [3], color octet technirhos [4], new gauge bosons W' and Z' [5], and E_6 diquarks [6]. The limit and theory curves require that both jets have pseudorapidity $|\eta| < 2.0$ and that the dijet system satisfies $|\cos \theta^*| < 2/3$.

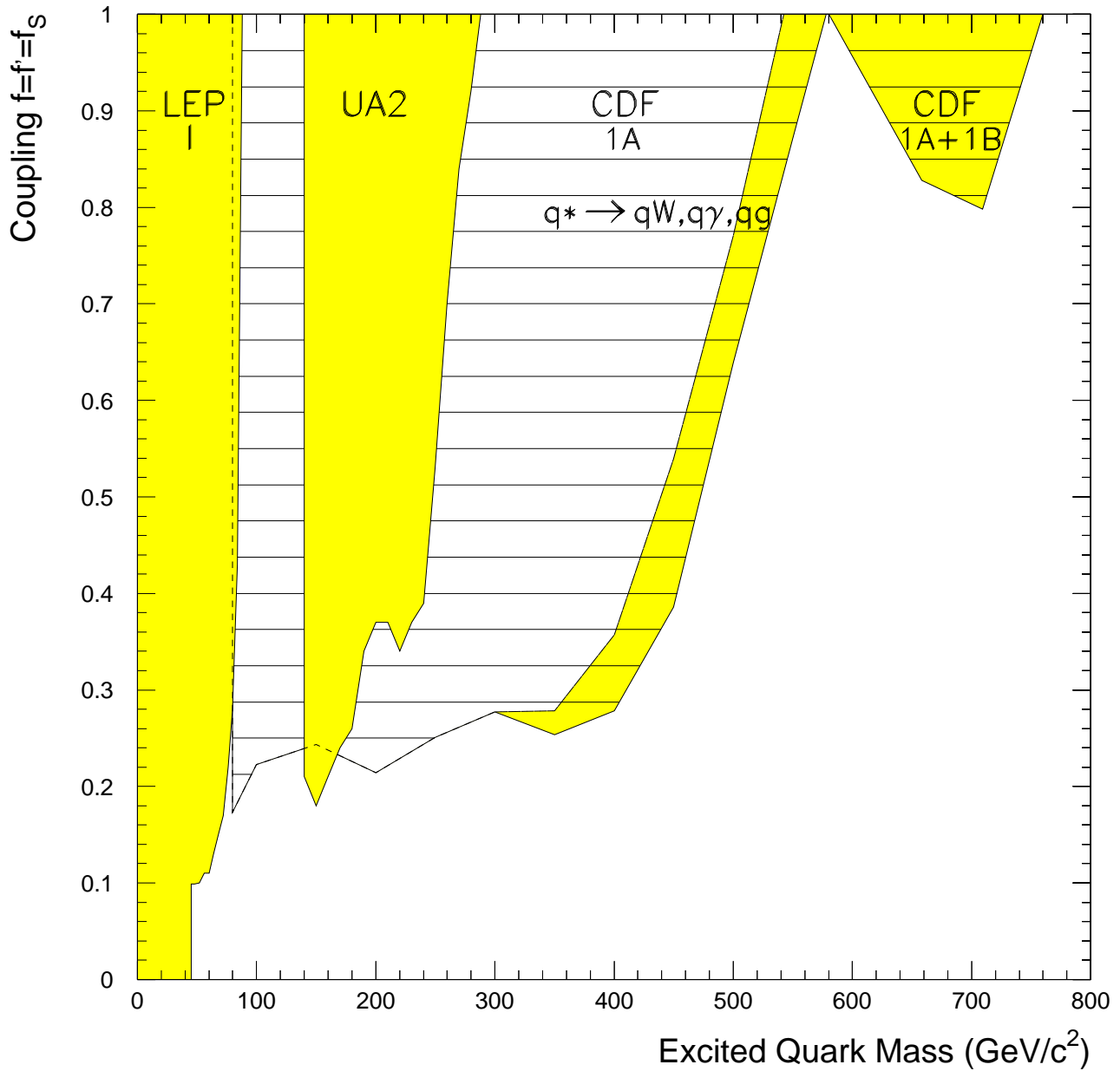


Figure 4: The region of the coupling vs. mass plane excluded by previous CDF measurements [1, 18] in the $q^* \rightarrow q\gamma$ and $q^* \rightarrow qW$ channels (clear hatched region) and $q^* \rightarrow qg$ channels (shaded hatched region on left) in run 1A is extended by this $q^* \rightarrow qg$ search in run 1A plus run 1B (shaded hatched region on right). The CDF excluded regions are compared to the regions excluded by LEP I and UA2 (shaded regions) [20].